Journal Pre-proofs

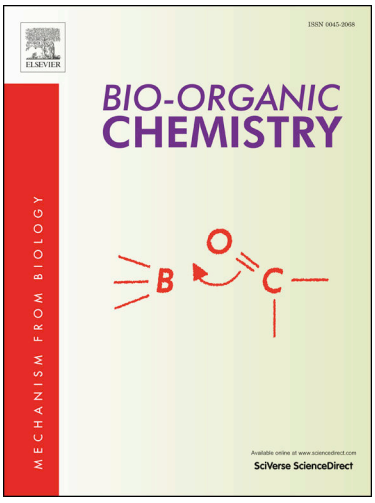

Discovery of 1,2,3-triazole based quinoxaline-1,4-di-*N*-oxide derivatives as potential anti-tubercular agents

Singireddi Srinivasarao, Adinarayana Nandikolla, Amaroju Suresh, Augustynowicz-Kopec Ewa, Agnieszka Głogowska, Balaram Ghosh, Banoth Karan Kumar, Sankaranarayanan Murugesan, Sravani Pulya, Himanshu Aggarwal, Kondapalli Venkata Gowri Chandra Sekhar

PII: S0045-2068(19)32256-4
DOI: https://doi.org/10.1016/j.bioorg.2020.103955
Reference: YBIOO 103955

To appear in: *Bioorganic Chemistry*

Received Date: 30 December 2019
Revised Date: 12 February 2020
Accepted Date: 17 May 2020

Please cite this article as: S. Srinivasarao, A. Nandikolla, A. Suresh, A-K. Ewa, A. Głogowska, B. Ghosh, B. Karan Kumar, S. Murugesan, S. Pulya, H. Aggarwal, K. Venkata Gowri Chandra Sekhar, Discovery of 1,2,3-triazole based quinoxaline-1,4-di-*N*-oxide derivatives as potential anti-tubercular agents, *Bioorganic Chemistry* (2020), doi: https://doi.org/10.1016/j.bioorg.2020.103955

Discovery of 1,2,3-triazole based quinoxaline-1,4-di-*N*-oxide derivatives as potential anti-tubercular agents

Singireddi Srinivasarao,[a] Adinarayana Nandikolla,[a] Amaroju Suresh,[a] Augustynowicz-Kopec Ewa,[b] Agnieszka Głogowska,[b] Balaram Ghosh,[c] Banoth Karan Kumar,[d] Sankaranarayanan Murugesan,[d] Sravani Pulya,[c] Himanshu Aggarwal[a] and Kondapalli Venkata Gowri Chandra Sekhar*[a]

[a]*Department of Chemistry, Birla Institute of Technology and Science, Pilani, Hyderabad Campus, Jawahar Nagar, Kapra Mandal, Hyderabad – 500 078, Telangana, India.*

[b]*Microbiology Department, National Tuberculosis and Lung Diseases Research Institute, 01-138 Warsaw, Poland.*

[c]*Department of Pharmacy, Birla Institute of Technology and Science, Pilani, Hyderabad Campus, Jawahar Nagar, Kapra Mandal, Hyderabad-500 078, Telangana, India.*

[d]*Medicinal Chemistry Research Laboratory, Department of Pharmacy, Birla Institute of Technology and Science, Pilani, 333 031, Rajasthan, India.*

Abstract: A series of thirty one novel 2-(((1-(substituted phenyl)-1*H*-1,2,3-triazol-4-yl)methoxy)carbonyl)-3-methylquinoxaline-1,4-dioxide (**7a-l**), 3-(((1-(substituted phenyl)-1*H*-1,2,3-triazol-4-yl)methoxy)carbonyl)-6-chloro-2-methylquinoxaline-1,4-dioxide (**8a-l**) and 2-(((1-(substituted phenyl)-1*H*-1,2,3-triazol-4-yl)methoxy)carbonyl)-6,7-dichloro-3-methylquinoxaline-1,4-dioxide (**9a-g**) analogues were synthesized, characterized using various analytical techniques and single crystal was developed for the compounds **8g** and **9f**. Synthesized compounds were evaluated for *in vitro* anti-tubercular activity against *Mycobacterium tuberculosis* H37Rv strain and two clinical isolates Spec. 210 and Spec. 192. The titled compounds exhibited minimum inhibitory concentration (MIC) ranging from 30.35 to 252.00 μM. Among the tested compounds, **8e**, **8l**, **9c** and **9d** exhibited moderate activity (MIC = 47.6 – 52.0 μM) and **8a** exhibited significant anti-tubercular activity (MIC = 30.35 μM). Furthermore, **8e**, **8l,** and **9d** were found to be less toxic against human embryonic kidney, HEK 293 cell lines. Finally, a docking study was also performed using MTB DNA Gyrase (PDB ID: 5BS8) for the significantly active compound **8a** to know the exact binding pattern within the active site of the target enzyme.

*Corresponding author

Tel.: +91 40 66303527 E-mail: kvgc@hyderabad.bits-pilani.ac.in; kvgcs.bits@gmail.com

Keywords: quinoxaline-1,4-di-N-oxide, 1,2,3-triazole, anti-mycobacterial activity, cytotoxicity.

1. Introduction

Mycobacterium tuberculosis is a pathogenic bacteria and causative agent of Tuberculosis (TB). TB is a contagious and infectious disease. Mostly, it affects the lungs (pulmonary TB) but can also affect other sites (extra pulmonary TB) in the body. TB remains the leading cause of death among infectious diseases worldwide. According to the 2019 WHO report it is estimated that 1.4 million people die throughout the world from TB [1].

Quinoxaline derivatives have a broad scope in medicinal chemistry as the compounds have diverse biological activities, such as antimicrobial, antiviral, anticancer, antifungal, and antitubercular [2-3]. In the last three decades, several quinoxaline derivatives like 2-oxo derivatives, mono, and di-*N*-oxide derivatives and their biological activities have been reported [4]. The pyrazine ring nitrogen, when oxidized, gives the quinoxaline-1,4-di-*N*-oxide. These *N*-oxides are endowed with antiviral, anticancer, antiprotozoal, and antibacterial activities [5-9]. Quinoxaline-1,4-di-*N*-oxide (**A**) is a common sub-structure of many biologically and pharmacologically active compounds. Several reports reveal that the compounds with various substituents at 2,3,6 and 7th position exhibit promising anti-TB activity (**B** to **G**) [5-16]. Pan *et al.* synthesized thirty-one compounds of quinoxaline-1,4-di-*N*-oxides variously substituted at the C-2 position, and their antimycobacterial MIC ranged from 0.39 to 50 μg/mL. From this reported work, **B** and **C** emerged to be the most active anti-TB agents with MTB MIC 0.39 and 1.56 μg/mL, respectively [10]. Sainza *et al.* reported quinoxaline-l,4-di-*N*-oxide derivatives with different substituents at 2,3,6 and 7th position as selective hypoxia agents. Some of these products gave good results as anti-tuberculosis agents [9-11]. 99% MTB inhibition was observed in different 7-chloro-3-(para-substituted) phenylaminoquinoxaline-2-carbonitrile-1,4-di-*N*-oxides [12] while 100 % growth inhibition was observed in 6,7-dichloro-2-(ethoxycarbonyl)-3-methylquinoxaline-1,4-dioxide and 3-acetamide-6,7-dichloroquinoxaline-2-carbonitrile-1,4-di-*N*-oxide derivatives [11,12]. Jaso *et al.* reported 2-acetyl and 2-benzoyl-6(7)-substituted quinoxaline-1,4-di-*N*-oxide derivatives with MTB MIC ranging from 3.3 to 62.5 μM against MTB H37Rv strains. Same group reported twenty-nine new 6 (7)-substituted quinoxaline-2-carboxylate-1,4-dioxides with MTB MIC ranging from 0.10 to >6.25 μg/mL [13-15]. Seven 2-benzoylquinoxaline-1,4-di-*N*-oxide derivatives and twenty-seven 2-acetylquinoxaline-1,4-di-*N*-oxides showed MTB MIC from 0.20 to 99.91 μg/mL against MTB H37Rv [15-16]. Torres *et al.,* reported 1,4-di-*N*-oxide-quinoxaline-2-ylmethylene isonicotinic acid hydrazides with MTB MIC

ranging from 0.58 to 90.84 μM against MTB H37Rv and **H** is the most potent agent with MTB MIC 0.58 μM [17]. Quinoxaline-*N*-oxide based anti-TB agents are depicted in **Figure 1**.

Recently, few selected derivatives were found to be active against the single drug-resistant strains of MTB and in macrophage model [17]. The two different molecules **F** and **G** were successful *in vivo* in a murine model. In non-replicating (NRP) bacteria, compounds **F** and **G** showed significant activity. If the action on NRP bacteria translates to *in vivo* conditions, it leads to shorter anti-TB treatment. Under this assumption, quinoxaline-1,4-di-*N*-oxides may represent a new class for very good orally active anti-TB drugs [18] with a potency to shorten the treatment period.

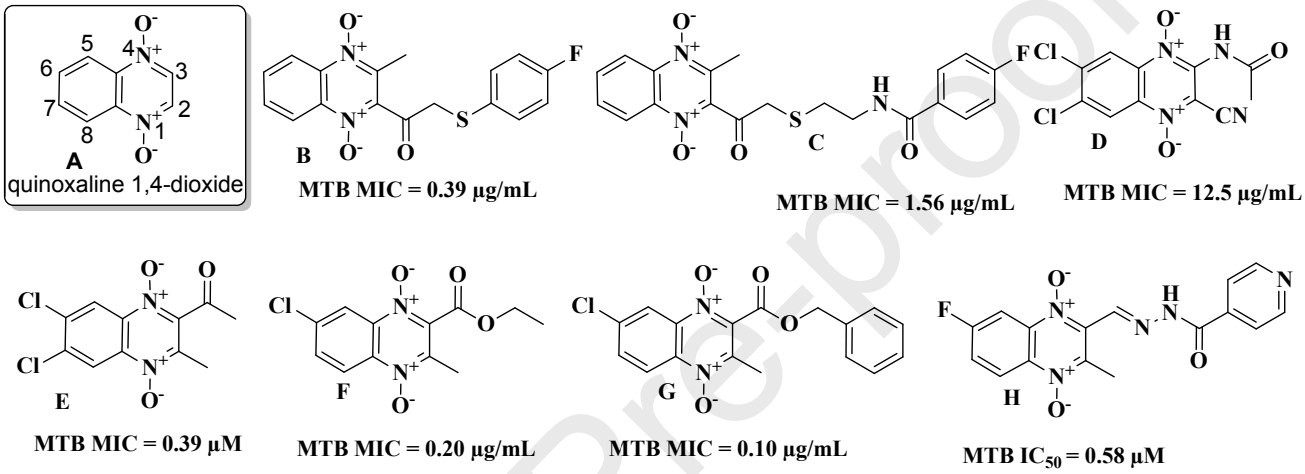

Figure 1: A is the numbering system in quinoxaline-1,4-dioxide and **B-H** are examples of *N*-oxide based anti-tubercular agents

1,2,3-triazole and their derivatives exhibited different biological activities viz., antibacterial, antifungal, antiviral, antiallergic, anti-HIV, anti-inflammatory, anticonvulsant, and β-Lactamase inhibition [19-22]. 1,2,3-triazole ring based compounds exhibit the dipole character moderately; they are rigid, capable of hydrogen bonding, and are also stable in *in vivo* conditions [23-24]. The *in vivo* and *in vitro* inhibitory activities of triazole based derivatives are very strong against MTB. To date, many triazole based anti-TB agents are published, and some of them (**I-N**) are showcased in **Figure 2** [25-29].

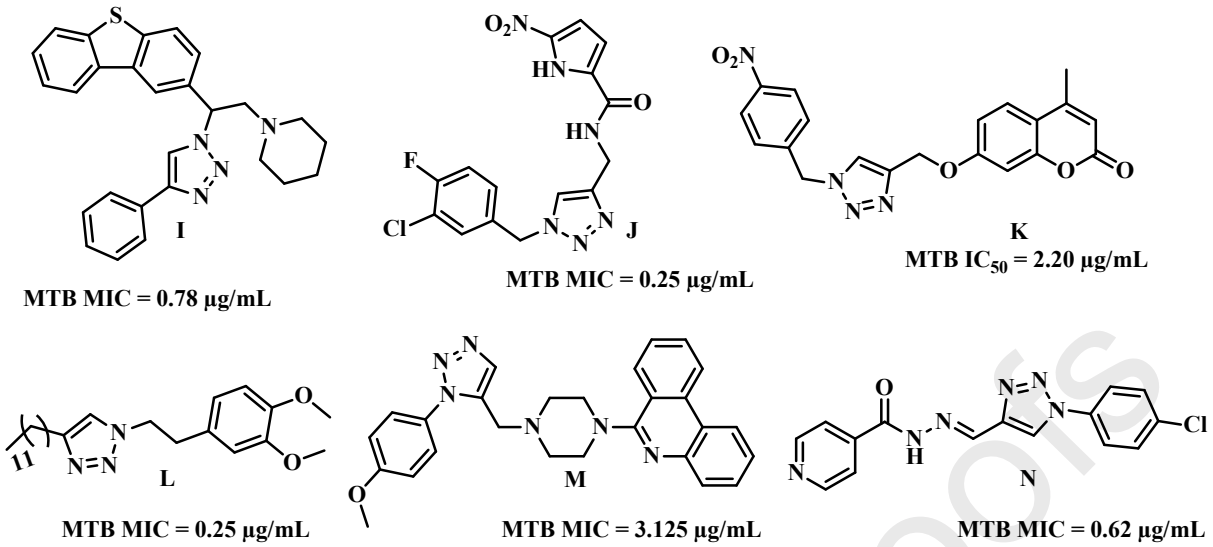

Figure 2: Some of the triazole based derivatives as anti-tubercular agents

Given the facts mentioned above about antitubercular activity observed in 1,2,3-triazoles and quinoxaline-1,4-di-*N*-oxides as well as in continuation to our ongoing efforts towards developing efficacious anti-TB agents, we designed the molecules of the current research work by hybridizing these two active heterocyclic systems together into a single entity as outlined in **Figure 3** [24]. We used ester linkage, as the compounds with ester group exhibited most promising anti-Tb activity (F and G of **Figure 1**) compared to other linkers. Various functionalities such as amide, alkyl and heterocycles can be varied. [30]

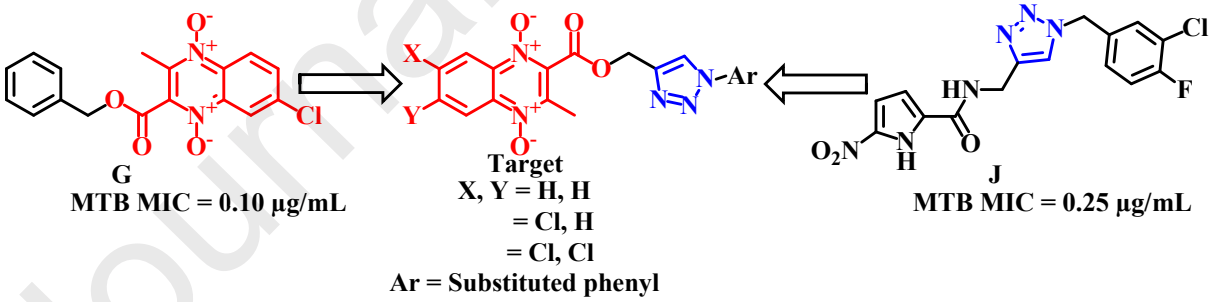

Figure 3: Synthetic strategy of the title compounds

2. Results and Discussion

Chemistry

The designed target molecules were synthesized in five steps (**Scheme-1**). Firstly, *N*-oxide intermediate (**3a-c**) was prepared *via* azides (**2a-c**). Ethyl acetoacetate was treated with propargyl

alcohol in toluene at 110 °C to get trans esterified compound **5**. Compound **5** on treatment with various substituted phenyl azides yielded 1*H*-1,2,3-triazoles (**6a-l**) [31]. Compound **6** upon reacting with various *N*-Oxide intermediates (**3a-c**) in the presence of triethylamine formed quinoxaline-1,4-dioxides **(7a-l, 8a-l,** and **9a-h)**. The synthesized compounds were purified, and structural elucidation was done with mass spectrometry, ^{1}H NMR and ^{13}C NMR. From NMR data, the respective signals of protons and carbons were verified with their coupling constants, multiplicities, and chemical shift values. The final reports nearly matched with the theoretical values within the range of ± 0.05.

Preparation of Intermediate 3a-c

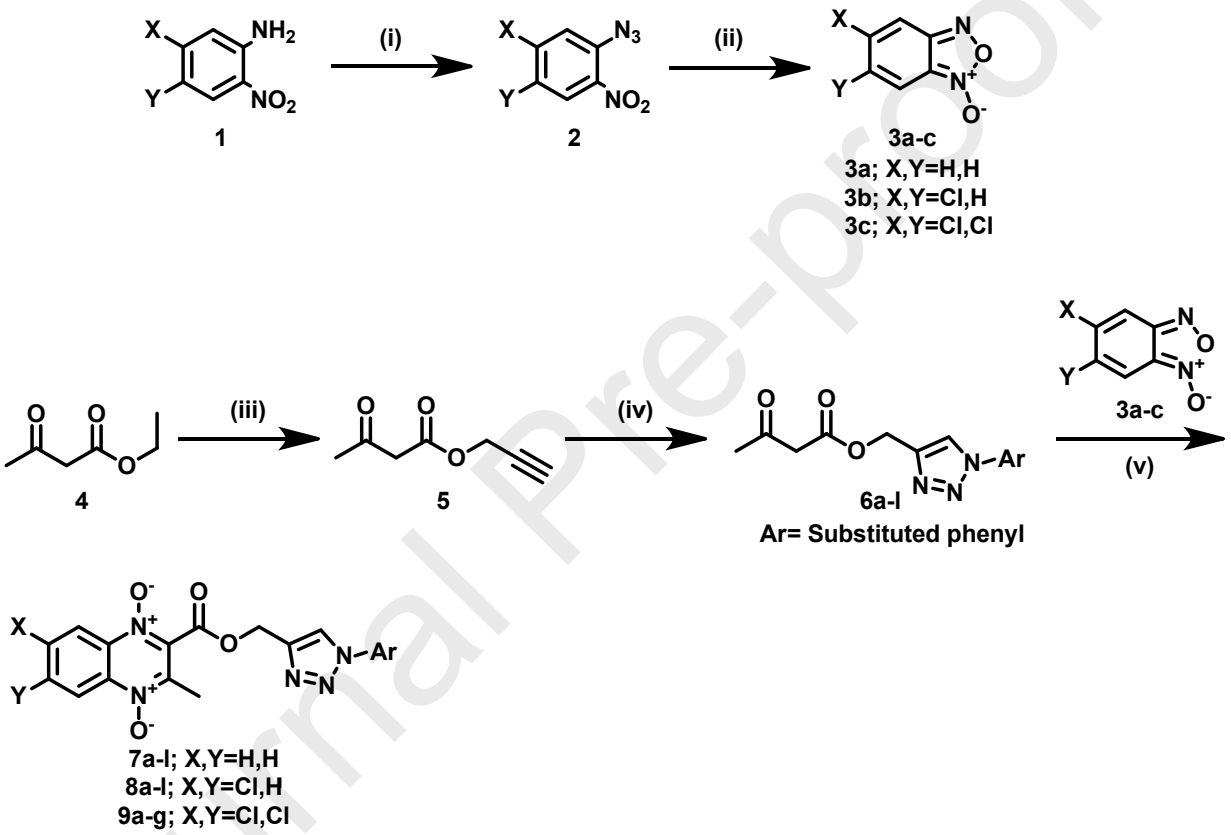

Scheme 1: Synthetic scheme of titled quinoxaline-1,4-di*N*-oxide derivatives

Reagents and conditions: (i) $NaNO_2$ (1.50 eq), NaN_3 (1.50eq), 6N HCl (8 wt/v), 0 °C, 2 h. (ii) toluene (30 wt/v), 110 °C, 24 h. (iii) propargyl alcohol (10.0eq), toluene, 24 h. (iv) substituted different aromatic azides, sodium ascorbate (10 mol %), CuI (10 mol%), $CuSO_4.5H_2O$ (10 mol %), ^{t}BuOH: H_2O (2:1), rt, 16 h. (v) *N*-oxide intermediate (**3a-c**) (1.2 eq), triethylamine, rt, 16 h.

In-vitro Mycobacterium tuberculosis **screening**

All the synthesized compounds were tested for their capacity to inhibit the growth of three different *M. tuberculosis* strains. Among the three, one of them was reference strain *M. tuberculosis H37Rv ATTC 25618*. The remaining were clinical strains isolated from TB patients [32-33]. MTB strain *spec. 210* was resistant to *p*-aminosalicylic acid, rifampicin, ethambutol, isoniazid (INH), while the other strain (*Spec. 192*) was fully sensitive to the administrated TB drugs [32]. The minimum inhibitory concentration (MIC) for the tested compounds was performed by a classical test-tube method of successive dilution in Youmans' modification of the Proskauer and Beck liquid medium containing 10% of bovine serum [33]. INH was taken as reference drug. The stock solutions of compounds and antibiotic were prepared in dimethyl sulfoxide (DMSO, Sigma Aldrich) and then diluted in liquid medium. The final concentrations of tested compounds and INH were in the range of 3.1–100 μg/ml. *Mycobacterium* strains were grown in Lowenstein-Jensen medium slants. Colonies were suspended with sterile distilled water containing 5 mm glass beads and vortexed during 45 s. The supernatant was harvested and adjusted to 0.5 McFarland (corresponding to approx. $1{,}5 \times 10^8$ CFU/ml) with a nephelometer (Becton, Dickinson & Company, Franklin Lakes, MD, USA). The, prepared inoculum was then added to each tube containing the tested compounds and antibiotics in various concentration, so the final inoculum size was $5x10^5$ CFU/ml. The test tubes were incubated at 37 °C for 21 days. The growth of mycobacteria was assessed using a visual method. The MIC value was determined as the lowest concentration of the drug at which no growth of microorganisms was observed (no turbidity). The negative and positive control consisted of medium without inoculum and medium inoculated with the same amount of bacteria respectively.

The result of *in vitro* studies on MTB is outlined in **Table 1**. The activity ranged from < 12.5 to > 100 μg/mL (30.35 to >252 μM).

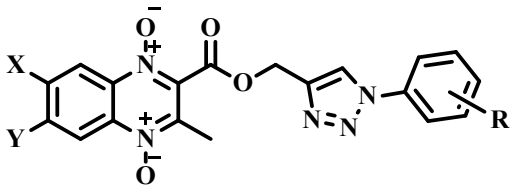

7(a-l); X,Y = H, H
8(a-l); X,Y = Cl, H
9(a-g); X,Y = Cl, Cl

Table 1: Results of antimycobacterial screening of titled compounds

Entry	X	Y	R	MIC µM (µg/mL) against MTB *H37Rv*	MIC µM (µg/mL) against MTB *Spec. 192*	MIC µM (µg/mL) against MTB *Spec. 210*
			Series-I			
7a	H	H	H	132.50 (50)	132.50 (50)	132.50 (50)
7b	H	H	4-Ethyl	123.33 (50)	123.33 (50)	123.33 (50)
7c	H	H	4-Fluoro	>252.94 (>100)	>252.94 (>100)	>252.94 (>100)
7d	H	H	4-Chloro	>242.84 (>100)	>242.84 (>100)	>242.84 (>100)
7e	H	H	4-Bromo	109.59 (50)	109.59 (50)	109.59 (50)
7f	H	H	4-nitro	>236.77 (>100)	>236.77 (>100)	>236.77 (>100)
7g	H	H	2- fluoro	126.47 (50)	126.47 (50)	126.47 (50)
7h	H	H	2-chloro	60.71 (25)	60.71 (25)	60.71 (25)
7i	H	H	2-nitro	59.19 (25)	59.19 (25)	59.19 (25)
7j	H	H	3-nitro	59.19 (25)	59.19 (25)	59.19 (25)
7k	H	H	3-trifluoromethyl	224.54 (100)	224.54 (100)	112.27 (50)
7l	H	H	3,5-dichloro	97.06 (50)	97.06 (50)	194.12 (100)
			Series-II			
8a	**Cl**	**H**	**H**	**30.35 (12.5)**	**30.35 (12.5)**	**30.35 (12.5)**
8b	Cl	H	4-ethyl	56.83 (25)	56.83 (25)	56.83 (25)
8c	Cl	H	4-fluoro	58.16 (25)	58.16 (25)	58.16 (25)
8d	Cl	H	4-chloro	56.02 (25)	56.02 (25)	56.02 (25)
8e	Cl	H	4-bromo	50.94 (25)	50.94 (25)	>203.76 (>100)
8f	Cl	H	4-nitro	54.72 (25)	54.72 (25)	54.72 (25)

8g	Cl	H	2-fluoro	58.16 (25)	58.16 (25)	58.16 (25)
8h	Cl	H	2-chloro	56.02 (25)	56.02 (25)	56.02 (25)
8i	Cl	H	2-nitro	54.72 (25)	54.72 (25)	109.44 (50)
8j	Cl	H	3-nitro	109.45 (50)	109.45 (50)	109.45 (50)
8k	Cl	H	3-trifluoromethyl	104.21 (50)	104.21 (50)	104.21 (50)
8l	Cl	H	3,5-dichloro	52.00 (25)	52.00 (25)	52.00 (25)
			Series-III			
9a	Cl	Cl	H	112.04 (50)	112.04 (50)	112.04 (50)
9b	Cl	Cl	4-fluoro	53.85 (25)	53.85 (25)	53.85 (25)
9c	Cl	Cl	4-chloro	52.00 (25)	52.00 (25)	52.00 (25)
9d	Cl	Cl	4-bromo	47.60 (25)	47.60 (25)	47.60 (25)
9e	Cl	Cl	2-fluoro	107.70 (50)	107.70 (50)	107.70 (50)
9f	Cl	Cl	2-chloro	104.01 (50)	104.01 (50)	104.01 (50)
9g	Cl	Cl	3,5-dichloro	97.06 (50)	97.06 (50)	97.06 (50)
Isoniazid	-	-	-	<22.59 (<3.1)	<22.59 (<3.1)	91.15 (12.5)

Among the thirty-one compounds screened, eight compounds **(8a, 8e, 8f, 8i, 8l, 9b, 9c** and **9d**) showed activity against MTB with MIC <55.00 µM. Two compounds (**8a** and **9d**) inhibited MTB with MIC <50.00 µM. Among these eight compounds, **8a** (6-chloro-2-methyl-3-(((1-phenyl-1*H*-1,2,3-triazol-4-yl)methoxy)carbonyl)quinoxaline-1,4-dioxide) is the most active one with MIC 30.35 µM.

SAR of compounds 7a-l

SAR is explained based on the activity of compound **7a**. Structural changes at the *ortho*, *meta,* and *para* positions alter the anti-TB activity. Compound **7a** was inhibiting the growth of MTB H37Rv strain at 132.50 µM. In this series, the introduction of an electron-donating ethyl group at the 4th position, activity remains unaltered. Presence of electron-withdrawing **F** and **Cl** on the phenyl ring at *para* position resulted in decrease in the activity by two folds (**7c**, MIC >252.94 µM; **7d,** MIC >242.84 µM) but the presence of bromo (**7e**) at *para* position increased the activity by one fold with MIC 109.59 µM. The presence of electron-withdrawing nitro group at *para* position decreased the activity by two folds (**7f**, >236.77 µM), but the nitro group at *ortho* and *meta* position increased the

activity by two folds (**7i,** MIC 59.19 μM; **7j,** MIC 59.19 μM). With the introduction of the fluoro group at the *ortho* position, activity remains unchanged compared to compound **7a,** but the presence of chloro (compound **7h**) at the *ortho* position enhanced the activity by two folds with MIC 60.71 μM. The presence of two **Cl** (compound **7l**) at 3rd and 5th position increased the activity by one fold with MIC 97.06 μM. The introduction of the electron-withdrawing CF_3 group (compound **7k**) at *meta* position decreased the activity by two folds with MIC 224.54 μM.

SAR of compounds 8a-l

SAR is explained based on the activity of compound **8a**. Compound **8a** was inhibiting the growth of MTB H37Rv strain at 30.35 μM. With the presence of electron-donating ethyl group at *para* position activity fell by two folds with MIC 56.83 μM. Introduction of electron-withdrawing groups *viz.,* **F, Cl,** and **Br** at the o*rtho, meta,* and *para* position, either mono or di-substituted resulted in a decrease in the activity by two folds. The presence of an electron-withdrawing nitro group at *para* position (compound **8f**) decreased the activity by two folds with MIC 54.72 μM while nitro group at *meta* position (compound **8j**) decreased the activity by four folds with MIC 109.45 μM. The introduction of the electron-withdrawing CF_3 group (compound **8k**) at *meta* position reduced the activity by four folds with MIC 104.21 μM. All these results showed that the insertion of electron-withdrawing moiety decreases the anti-tubercular activity.

SAR of compounds 9a-g

In this series, two **Cl** groups were introduced on the quinoxaline-1,4-*N*-dioxide frame. SAR is explained based on the activity of compound **9a** (MIC 112.04 μM). With introduction of electron-withdrawing halogens like *viz.,* **F, Cl,** and **Br** at *para* position on the phenyl moiety, activity increased by two folds (**9b,** MIC 53.85 μM; **9c,** MIC 52.00 μM, and **9d,** MIC 47.60 μM) but presence of **F** and **Cl** at the *ortho* position, activity remains unchanged (**9e,** MIC 107.70 μM; **9f,** MIC 104.01 μM). The introduction of Cl at 3rd and 5th positions resulted in the retention of the activity. The presence of two Cls on quinoxaline-1,4-*N*-dioxide did not improve the anti-TB activity. Overall, it was noticed that 6-chloro-3-(((1-(substituted phenyl)-1*H*-1,2,3-triazol-4-yl)methoxy)carbonyl)-2-methylquinoxaline-1,4-dioxide derivatives (**8a-l**) exhibited better anti-TB activity followed by 2-(((1-(substituted phenyl)-1*H*-1,2,3-triazol-4-yl)methoxy)carbonyl)-3-methylquinoxaline-1,4-dioxide derivative (**7a-l**) and 6,7-dichloro-2-(((1-(4-fluorophenyl)-1*H*-1,2,3-triazol-4-yl)methoxy)carbonyl)-3-methylquinoxaline-1,4-dioxide derivatives (**9a-g**). The schematic representation of SAR studies is showed in **Figure 4.**

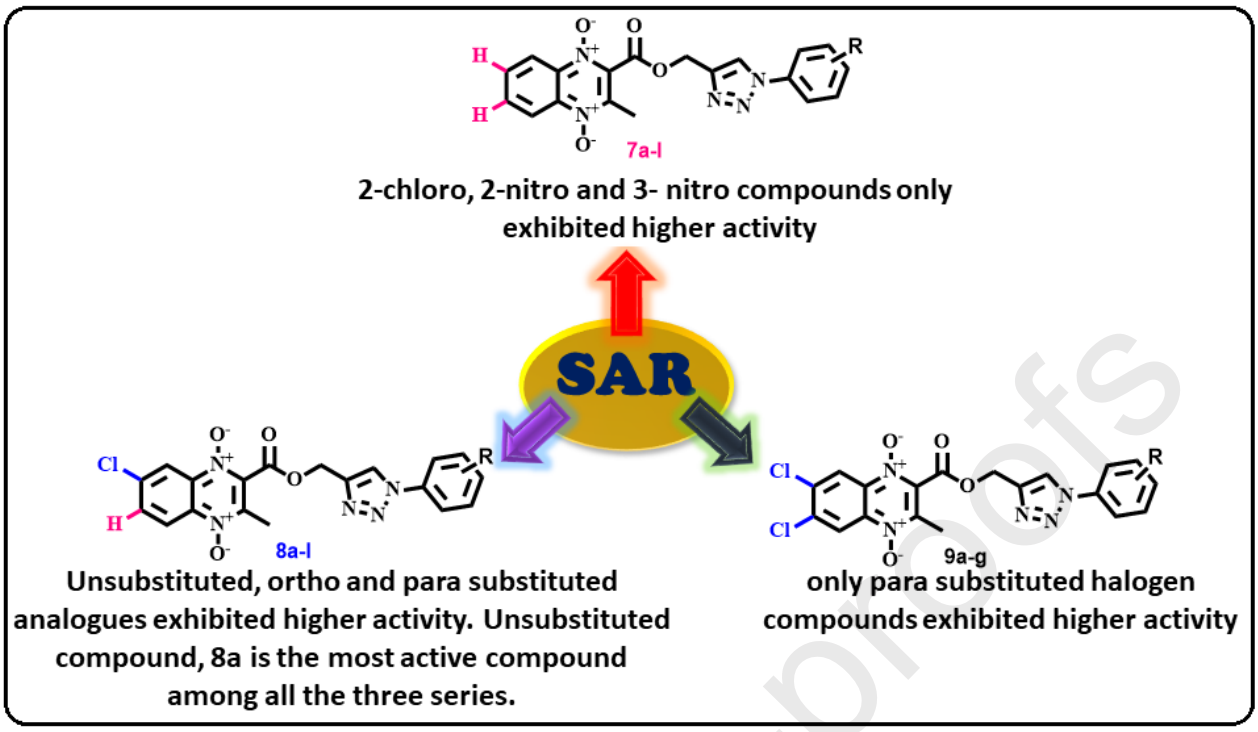

Figure 4: Structural activity relationship of the three series of compounds.

***In-silico* predicted physicochemical properties**

Currently, before approval of the drug into the market, ADMET properties of the drugs should be in the optimum range. These parameters play a crucial role in the physicochemical properties of the drugs after administration. To predict these parameters, several online servers / commercial softwares were available [34]. QikProp [35-36] (commercial software with Schrodinger) was used for the prediction of physico-chemical parameters of the titled new chemical entities. The significant parameters were considered related to the Lipinski rule (Rule of five) and Jorgensen's rule of three [37] (descriptions of these rules is described in **Table 2**).

All the titled compounds possessed the predicted physicochemical properties within the acceptable range as that of most of the marketed drugs. These compounds satisfy all the parameters related to the Lipinski rule of five (except compound **9g** in terms of molecular weight and log $P_{o/w}$). Jorgensen's rule of three was also satisfied with the same set of compounds. Very few compounds violated the solubility parameters (**7j, 7i, 7g, 7f,** and **7a**). Overall, all the predicted parameters were well within the range, and these compounds are not likely to encounter any problem in further development, if any.

Table-2. *In-silico* predicted parameters of the titled compounds

		Lipinski rule					Jorgensen's rule of three		
Code	**MW**	**Donor HB**	**Accept HB**	**Log $P_{o/w}$**	**Violation**	**LogS**	**Metabolites**	**PCaco**	**Violations**
7a	377.36	0	6	3.28	0	-5.294	4	268.328	0
7b	405.41	0	6	3.95	0	-6.295	5	258.554	1
7c	395.35	0	6	3.53	0	-5.694	4	266.316	0
7d	411.8	0	6	3.79	0	-6.066	4	268.041	1
7e	456.26	0	6	3.86	0	-6.181	4	267.175	1
7f	422.36	0	7	2.58	1	-5.256	5	41.28	0
7g	395.35	0	6	3.51	0	-5.431	4	353.9	0
7h	411.8	0	6	3.84	0	-5.884	4	385.357	1
7i	422.36	0	7	2.7	1	-5.175	5	58.119	0
7j	422.36	0	7	2.48	1	-5.209	5	30.889	0
7k	445.36	0	6	4.6	0	-7.611	5	265.59	1
7l	446.25	0	6	4.3	0	-6.849	4	271.01	1
8a	411.8	0	6	3.79	0	-6.055	3	271.704	1
8b	439.86	0	6	4.45	0	-7.059	4	258.858	1
8c	429.79	0	6	4.03	0	-6.459	3	266.798	1
8d	446.25	0	6	4.29	0	-6.823	3	271.002	1
8e	490.7	0	6	4.37	0	-6.943	3	270.977	1
8f	456.8	0	7	3.08	1	-6.003	4	41.78	1
8g	429.79	0	6	4.02	0	-6.226	3	353.202	1
8h	446.25	0	6	4.35	0	-6.655	3	383.477	1
8i	456.8	0	7	3.2	1	-5.933	4	58.344	1
8j	456.8	0	7	3.01	1	-6.086	4	30.881	1
8k	479.8	0	6	4.79	0	-7.557	4	267.721	1
8l	480.69	0	6	4.82	0	-7.555	3	293.281	1
9a	446.25	0	6	4.23	0	-6.701	2	270.93	1
9b	464.24	0	6	4.48	0	-7.135	2	271.547	1
9c	480.69	0	6	4.73	0	-7.474	2	269.907	1
9d	525.15	0	6	4.81	1	-7.577	2	273.194	1
9e	464.24	0	6	4.46	0	-6.846	2	354.703	1
9f	480.69	0	6	4.78	0	-7.28	2	385.653	1
9g	515.14	0	6	5.25	2	-8.261	2	270.129	1

Description: Lipinski rule- *Number of violations of Lipinski's rule of five. The rules are: mol MW < 500, logPo/w < 5, donor HB ≤ 5, accept HB ≤ 10 and maximum 4 violations*

Jorgensen's rule of three *- Number of violations of Jorgensen's rule of three. The three rules are: logS> -5.7, PCaco> 22 nm/s, # Primary Metabolites < 7. Compounds with fewer (maximum 3) violations*

In-silico molecular docking studies

Docking studies of the significantly active molecule (**8a**) was performed using the Glide module [38] in Schrodinger. All docking calculations were performed using Extra Precision (XP) mode. A scaling factor of 0.8 and a partial atomic charge of less than 0.15 was applied to the atoms of the

protein. Glide docking score (**Table 3**) was used to determine the best-docked structure from the output. The interactions of these docked complexes were investigated further by using XP visualizer.

Validation of the docking protocol

The accuracy of the docking study was determined by finding the lowest energy conformation of the co-crystallized ligand and resembles an experimental binding mode as determined by X-ray crystallography. The docking procedure was verified by removing the co-crystallized ligand from the binding site of the protein and re-docked the same co-crystallized ligand in the active binding site. The hydrogen-bonding interactions and RMSD between the anticipated confirmation and the observed X-ray crystallographic conformation was used for validation of the docking protocol. The RMSD for the targeted protein was found to be 0.46A^{o} (**Figure 5**) indicated that the docking protocol could be reliable for further study and ready for the docking of titled compounds.

Table-3. Scrutiny of amino-acid residues and water molecules contributed to the interactions with the targeted protein- 5BS8

Code (PDB – 5BS8)	H-bond Interactions	Halogen bond	Glide score (kcal/mol)	Glide energy (kcal/mol)
8a	-	ARG-128 ARG-128	-7.4	-48.5
Co-crystallized ligand (Moxifloxacin)	ARG-128 ARG-128 *HOH-205,206,209,210	ARG-128 (Salt bridge)	-11.5	-67.7

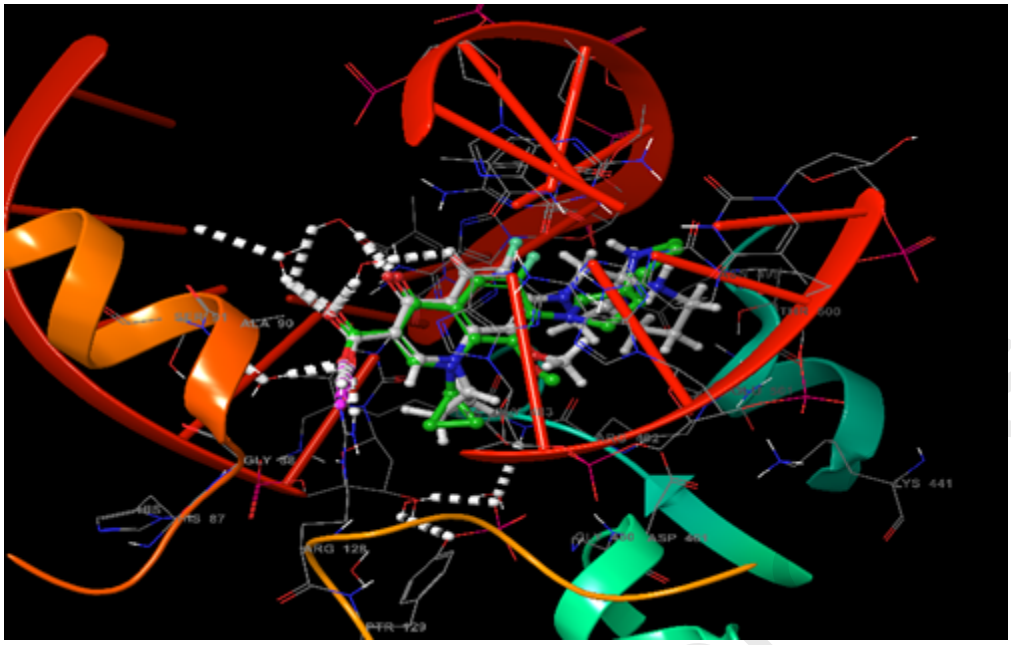

Figure 5. Superimposed view of the co-crystallized ligand in the active site of the protein -5BS8 (Green color- Binding pose after docking, White color- X-ray native pose of ligand)

Figure 6. Co-crystallized ligand (Moxifloxacin) docked pose and interactions in the active site of the protein-5BS8. *[Color interpretation White- Hydrogen bond, Magenta – Salt bridge.*

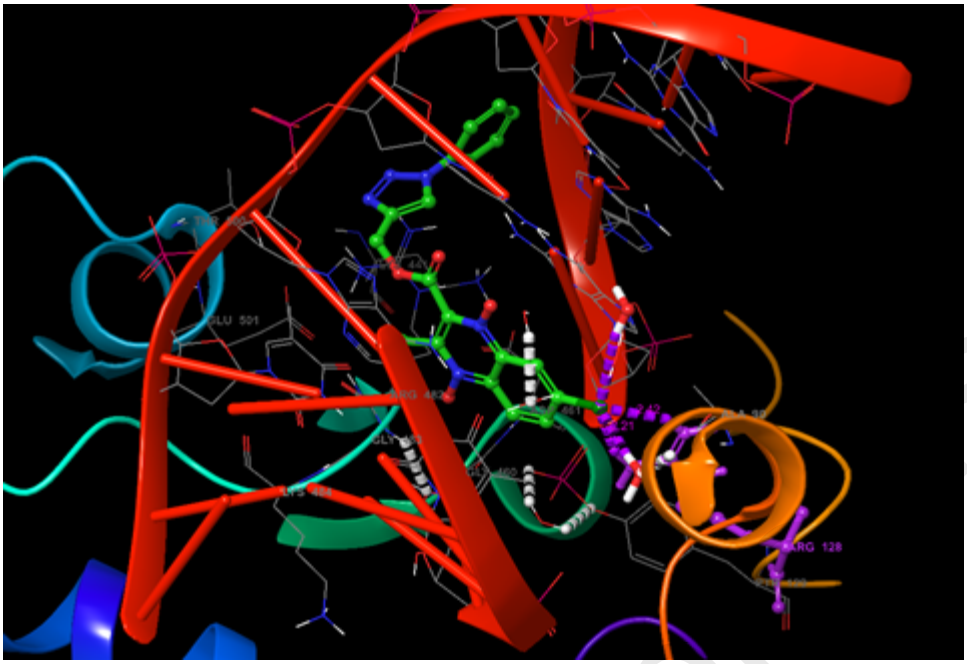

Figure 7. Significantly active compound **8a** docked pose and interactions in the active site of the protein-5BS8. [Color interpretation: Purple- Halogen bond]

The docking score of the significantly active compound **8a** is low (Glide score-7.4 kcal/mol) as compared with the co-crystallized ligand (Moxifloxacin) (Glide score -11.5 kcal/mol) (**Table 3**). Analyzing the interactions of the molecule in the target protein revealed that the co-crystallized ligand (**Figure 6**) showed one hydrogen bond interaction with the surrounded four water molecules as well as another hydrogen bond interaction with amino acid residue ARG-128 of the target protein. However, the significantly active molecule **8a** exhibited two halogen bond interactions (**Figure 7**) with the amino acid residue ARG-128 of the target protein and no hydrogen bond interactions as that of the co-crystallized ligand. This might be the possible reason for the reduced docking score of the significantly active moiety. Docking study and *in-vitro* anti-tubercular activity studies are correlating the results. The significantly active compound exhibited the minimum inhibitory concentration of 30.35 µM among the titled compounds tested against all the mycobacterial cell lines i.e. MTB *H37Rv,* MTB *Spec 192*, MTB *Spec 210.*

Single crystal X-ray crystallographic structure of compounds 8g and 9f

The suitable crystals of compounds **8g** and **9f** for single-crystal X-ray diffraction (SCXRD) study were grown from the mixture of methanol and dichloromethane (1:3). The SCXRD measurements were performed on the Rigaku XtaLAB P200 diffractometer using graphite monochromated Cu-Kα

radiation (λ = 1.54184 Å). The data was collected and reduced using CrysAlisPro (Rigaku Oxford Diffraction) software. The data collection was carried out at 100 K, and the structures were solved using Olex2 with the ShelX structure solution program using Direct Methods and refined with the ShelXL refinement package using Least Squares minimization. The primary crystallographic data are shown in **Table 4**.

The molecular structure of the compound **8g** contains one linker per asymmetric unit (**Figure 8**) with the chemical formula ($C_{19}H_{12}ClFN_5O_4$), where one of the chlorine atoms (Cl3) has 80% occupancy whereas the second chlorine atom (Cl4) has 20% occupancy. The structure crystallizes in the monoclinic crystal system. On the other hand, the compound **9f** crystallizes in the triclinic crystal system, where two linkers are observed per asymmetric unit (**Figure 8**). Crystallographic data for the compounds **8g** and **9f** has been deposited to the Cambridge Crystallographic Data Center, and the corresponding deposition number is **CCDC 1913106** and **1937576**, respectively.

Table 4. Crystal data and structure refinement for compounds **8g** and **9f**

Identification code	**8g**	**9f**
Empirical formula	$C_{19}H_{12}N_5O_4ClF$	$C_{19}H_{12}N_5O_4Cl_3$
Formula weight	428.790	480.70
Temperature/K	293	100.0
Crystal system	Monoclinic	triclinic
Space group	I 2/a	P-1
a/Å	29.8337(7)	4.73450(10)
b/Å	4.7387(1)	17.2736(2)
c/Å	27.6372(7)	23.9809(3)
α/°	90.000	92.3020(10)
β/°	110.662(3)	90.8230(10)
γ/°	90.000	96.7280(10)
Volume/Å^3	3655.8(2)	1945.77(5)
Z	8	4
ρ_{calc}g/cm^3	1.558	1.6408
μ/mm^{-1}	2.305	4.629
F(000)	1752	983.2
Crystal size/mm^3	0.02 × 0.02 × 0.3	0.3 × 0.05 × 0.02
Radiation	Cu Kα (λ = 1.54184)	Cu Kα (λ = 1.54184)
2Θ range for data collection/°	10.6 to 159.8	8.82 to 160
Index ranges	-37 ≤ h ≤ 35, -4 ≤ k ≤ 5, -34 ≤ l ≤ 34	-5 ≤ h ≤ 3, -21 ≤ k ≤ 21, -30 ≤ l ≤ 30
Reflections collected	9797	23507
Independent reflections	3823 [R_{int} = 0.0284, R_{sigma} =	8200 [R_{int} = 0.0409, R_{sigma} =

	0.0513]	0.0422]
Data/restraints/parameters	3823/0/281	8200/0/561
Goodness-of-fit on F^2	1.092	1.014
Final R indexes [I>=2σ (I)]	$R_1 = 0.0633$, $wR_2 = 0.1429$	$R_1 = 0.0399$, $wR_2 = 0.1058$

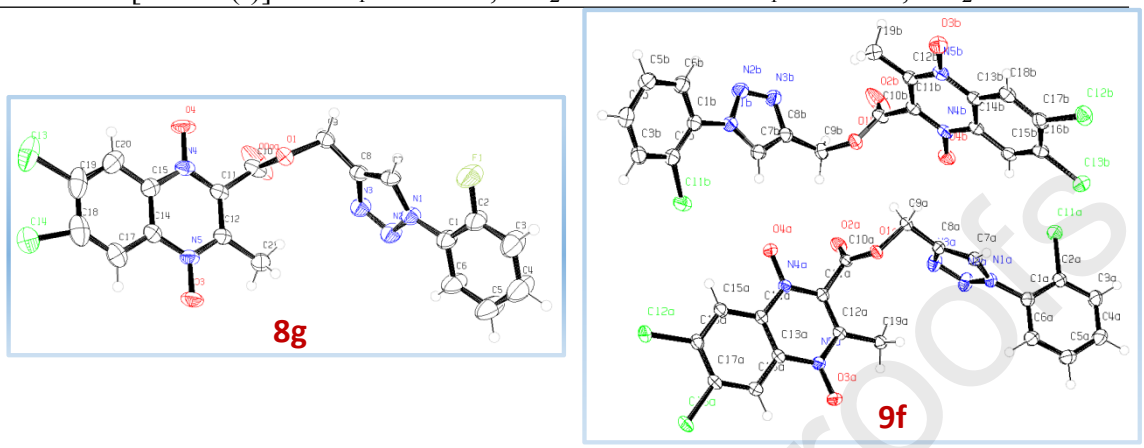

Figure 8. ORTEP diagram of crystals **8g** and **9f**

***In vitro* cytotoxicity studies**

Compounds with MTB MIC < 60 µM (**7h, 7i, 7j, 8a, 8e, 8f, 8i, 8l, 9b, 9c,** and **9d)** were subjected to cytotoxicity studies against normal human cell lines, human embryonic kidney (HEK) cells. Cell viability was measured by *in vitro* MTT assay [39]. Cells were exposed to compound treatment at a range of concentrations 2000, 1000, 500, 250, 125, 62.5, 31.25, 15.62, and 7.81 µM to determine their IC_{50} values from the dose-response curve. Data represent mean values of measurements ± s.d. (**Figure 9**). The obtained result clearly indicates selectivity of the compounds for mycobacterium

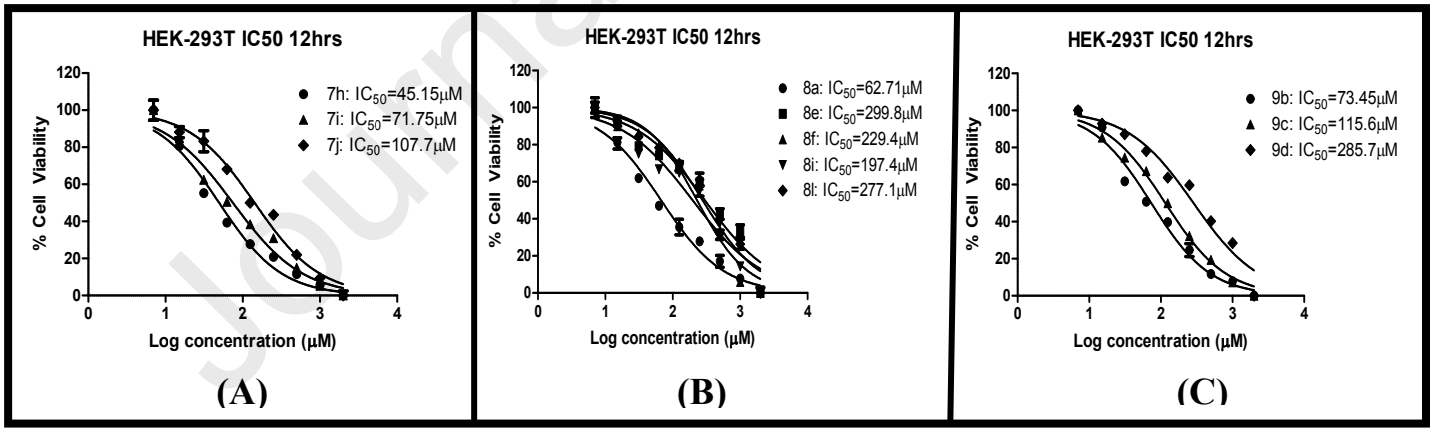

over normal cell lines. The most potent compound **8a** (100% bacterial inhibition concentration, MIC = 30.35 µM) showed significant selectivity towards MTB over HEK cells (HEK IC_{50} = 62.71 µM, IC_{100} = 125.42 µM, bacterial MIC = 30.35 µM; selective = 125.42/30.35 = ~ 4 fold) and that the remaining compounds were even more selective for bacterial cells over normal human cell lines.

Figure 9: IC_{50} results of the 11 compounds by MTT assay. Graph **(A)** represents the IC_{50} values for **7h**, **7i**, **7j** , Graph **(B)** represents the IC_{50} values for **8a**,**8e**,**8f**,**8i**,**8l** and graph **(C)** represents the IC_{50} values for **9b**,**9c**,**9d** on HEK-293T cells when treated with the compounds at concentration range of 7-2000 μM (n=2) for 12 hrs. Data represents mean ±SD.

3. Conclusion

In this work, quinoxaline-1,4-di-*N*-oxide analogues with three different series were synthesized; 2-methyl-3-(((substituted phenyl)-1*H*-1,2,3-triazol-4-yl)methoxy)carbonyl)quinoxaline-1,4-di-*N*-oxide derivatives, 6-chloro-3-(((1-(substituted phenyl)-1*H*-1,2,3-triazol-4-yl)methoxy)carbonyl)-2-methylquinoxaline-1,4-di-*N*-oxide derivatives and 6,7-dichloro-2-(((1-(4-fluorophenyl)-1*H*-1,2,3-triazol-4-yl)methoxy)carbonyl)-3-methylquinoxaline-1,4-di-*N*-oxide derivatives by molecular hybridization approach. Amongst the synthesized compounds, 6-chloro-3-(((1-(substituted phenyl)-1*H*-1,2,3-triazol-4-yl)methoxy)carbonyl)-2-methylquinoxaline-1,4-di-*N*-oxide derivatives showed significant anti-TB results. One of the compounds, **8a,** showed excellent MTB activity with MIC 30.35 μM. Further, the few most active compounds in the series did not exhibit high cytotoxicity against HEK cell lines. Finally, the significantly active compound, standard drug, and co-crystallized ligands were subjected to molecular docking studies to explore their putative binding interaction pattern at the active site of MTB DNA Gyrase.

Supporting information summary

Experimental procedures for intermediates (chemistry) and spectroscopic / analytical data along with representative ^{1}HNMR and ^{13}CNMR spectra are available in supporting information.

Acknowledgements

KVGCS and SM thank DBT, New Delhi [BT/IN/Spain/39/SMl2017-18] for providing financial support. The financial assistance provided by DIST FIST grant (SR/FST/CSI-240/2012), New Delhi is gratefully acknowledged. SS thanks CSIR for providing SRF fellowship. Central analytical lab facilities of BITS Pilani Hyderabad campus are gratefully acknowledged.

References

[1] https://www.who.int/tb/publications/global_report/en/

[2] G.W.H. Cheeseman, R.F. Cookson, Chemistry of Heterocyclic Compounds: Condensed Pyrazines, Chem. Heterocycl. Compd, 35 (1979) 1–27. https://doi.org/10.1002/9780470187333.

[3] A.E.A. Porter, in: A.R. Katrizky, C.W. Rees (Eds.), Comprehensive Heterocyclic Chemistry, vol. 3, Pergamon Press, New York, 1984.

[4] A. Carta, G. Pagliettia, M.E.R. Nikookar, P. Sanna, L. Sechi, S. Zanetti, Novel substituted quinoxaline 1,4-dioxides with *in vitro* antimycobacterial and anticandida activity, Eur. J. Med. Chem. 37 (5) (2002) 355-366. https://doi.org/10.1016/S0223-5234(02)01346-6.

[5] E. Vicente, R. Villar, B. Solano, A. Burguete, S. Ancizu, S. Pérez-Silanes, I. Aldana and A. Monge, Derivados de 1,4-di-N-óxido de quinoxalinayenfermedades olvidadas, A. An. R. Acad. Nac. Farm., 73 (4) (2007) 927-945. http://hdl.handle.net/10171/29525.

[6] G. Aguirre, H. Cerecetto, R. Di Maio, M. Gonzalez, M.E.M. Alfaro, A. Jaso, B. Zarranz, M.A. Ortega, I. Aldana, A.M. Vega, Quinoxaline *N*,*N*′-dioxide derivatives and related compounds as growth inhibitors of *Trypanosoma cruzi*. Structure–activity relationships, Bioorg. Med. Chem. Lett. 14 (14) (2004) 3835-3839. https://doi.org/10.1016/j.bmcl.2004.04.088.

[7] C. Urquiola, M. Vieites, G. Aguirre, A. Marin, B. Solano, G. Arrambide, P. Noblia, M.L. Lavaggi, M.H. Torre, M. Gonzalez, A. Monge, D. Gambino, H. Cerecetto, Improving anti-trypanosomal activity of 3-aminoquinoxaline-2-carbonitrile N-1,N4-dioxide derivatives by complexation with vanadium, Bioorg. Med. Chem., 14 (16) (2006) 5503-5509. https://doi.org/10.1016/j.bmc.2006.04.041.

[8] A. Carta, M. Loriga, G. Paglietti, A. Mattana, P. L. Fiori, P. Mollicotti, L. Sechi and S. Zanetti, Synthesis, anti-mycobacterial, anti-trichomonas and anti-candida in vitro activities of 2-substituted-6,7-difluoro-3-methylquinoxaline 1,4-dioxides, Eur. J. Med. Chem., 39 (2) 2004 195-203. https://doi.org/10.1016/j.ejmech.2003.11.008.

[9] B. Ganley, G. Chowdhury, J. Bhansali, J.S. Daniels, K.S. Gates, Redox-activated, hypoxia-selective DNA cleavage by quinoxaline 1,4-di-*N*-oxide, Bioorg. Med. Chem., 9 (9) 2001, 2395-2401. https://doi.org/10.1016/S0968-0896(01)00163-8.

[10] Y. Pan, P. Li, S. Xie, Y. Tao, D. Chen, M. Dai, H. Hao, L. Huang, Y. Wang, L. Wang, Z. Liu, Z. Yuan, Synthesis, 3D-QSAR analysis and biological evaluation of quinoxaline 1,4-di-*N*-oxide derivatives as antituberculosis agents, Bioorg. Med. Chem. Lett. 26 (16) 2016 4146-4153. https://doi.org/10.1016/j.bmcl.2016.01.066.

[11] Y. Sainza, M. E. Montoya, F. J. Martínez-Crespo, M. A. Ortega, A. L. de Ceráin and A. Monge, New Quinoxaline 1,4-Di-N-oxides for Treatment of Tuberculosis, Arzneimittelforschung. 49 (1) (1999) 55-59. https://doi.org/10.1055/s-0031-1300359.

[12] M. A. Ortega, Y. Sainz, M. E. Montoya, A. López de Ceráin, and A. Monge, Die Pharmazie, Synthesis and antituberculosis activity of new 2-quinoxalinecarbonitrile 1,4-di-N-oxides, 54 (1) 1999 24-25. https://doi.org/10.1002/chin.199921160.

[13] B. Zarranz, A. Jaso, I. Aldana, A. Monge, Synthesis and antimycobacterial activity of new quinoxaline-2-carboxamide 1,4-di-N-oxide derivatives, Bioorg Med Chem. 11 (10) (2003) 2149-2156. https://doi.org/10.1016/S0968-0896(03)00119-6.

[14] A. Jaso, B. Zarranz, I. Aldana, A. Monge, Synthesis of new 2-acetyl and 2-benzoyl quinoxaline 1,4-di-*N*-oxide derivatives as anti-*Mycobacterium tuberculosis* agents, Eur. J. Med. Chem. 38 (9) (2003) 791-800. https://doi.org/10.1016/S0223-5234(03)00137-5.

[15] A. Jaso, B. Zarranz, I. Aldana, A. Monge, Synthesis of New Quinoxaline-2-carboxylate 1,4-Dioxide Derivatives as anti-*Mycobacterium tuberculosis* Agents, J. Med. Chem. 48(6) (2005) 2019-2025. https://doi.org/10.1021/jm049952w.

[16] E. Moreno, S.P. Silanes, S. Gouravaram, A. Macharam, S. Ancizu, E. Torres, I. Aldana, A. Monge and P.W. Crawford, 1,4-Di-*N*-oxide quinoxaline-2-carboxamide: Cyclic voltammetry and relationship between electrochemical behavior, structure and anti-tuberculosis activity, Electrochim. Acta. 56 (9) (2011) 3270-3275. https://doi.org/10.1016/j.electacta.2011.01.030.

[17] E. Torres, E. Moreno, S. Ancizu, C. Barea, S. Galiano, I. Aldana, A. Monge, S.P. Silanes, New 1,4-di-*N*-oxide-quinoxaline-2-ylmethylene isonicotinic acid hydrazide derivatives as anti-*Mycobacterium tuberculosis* agents, Bioorg. Med. Chem. Lett. 21 (12) (2011) 3699-3703, https://doi.org/10.1016/j.bmcl.2011.04.072.

[18] E. Vicente, R.Villar,S.Pérez-Silanes, I. Aldana, R. C. Goldman, A. Monge, Quinoxaline 1,4-di-N-Oxide and the Potential for Treating Tuberculosis, Infectious Disorders – Drug Targets.11 (9) (2011) 196-204. https://doi.org/10.2174/187152611795589735.

[19] W. Zhang, Z. Li, M. Zhou, F. Wu, X. Hou, H. Luo, H. Liu, X. Han, G. Yan, Z. Ding, R. Li, Synthesis and biological evaluation of 4-(1,2,3-triazol-1-yl)coumarin derivatives as potential antitumor agents, Bioorg. Med. Chem. Lett., 24 (3) (2014) 799-807. https://doi.org/10.1016/j.bmcl.2013.12.095.

[20] M.J. Giffin, H. Heaslet, A. Brik, Y.C. Lin, G. Cauvi, C.H. Wong, D.E. McRee, J.H. Elder, C.D. Stout and B.E. Torbett, A Copper(I)-Catalyzed 1,2,3-Triazole Azide−Alkyne Click Compound

Is a Potent Inhibitor of a Multidrug-Resistant HIV-1 Protease Variant, J. Med. Chem., 51 (20) (2008) 6263-6270. https://doi.org/10.1021/jm800149m.

[21] Z.C. Dai, Y.F. Chen, M. Zhang, S.K. Li, T.T. Yang, L. Shen, J.X. Wang, S.S. Qian, H.L. Zhu, Y.H. Ye, Synthesis and antifungal activity of 1,2,3-triazole phenylhydrazone derivatives, Org. Biomol. Chem. 13(2) (2015) 477-486. https://doi.org/10.1039/C4OB01758G

[22] D.R. Buckle, C.J.M. Rockell, H. Smith, B.A. Spicer, Studies on 1,2,3-triazoles. 13. (Piperazinylalkoxy)-[1]benzopyrano[2,3-d]-1,2,3-triazol-9(1H)-ones with combined H1-antihistamine and mast cell stabilizing properties, J. Med. Chem., 29 (11) (1986) 2262-2267. https://doi.org/10.1021/jm00161a022.

[23] H.C. Kolb, K.B. Sharpless, The growing impact of click chemistry on drug discovery, Drug Discov. Today. 8 (24) 2003, 1128-1137. https://doi.org/10.1016/S1359-6446(03)02933-7.

[24] R.S. Keri, S.A. Patil, S. Budagumpi, B.M. Nagaraj, Triazole: A Promising Antitubercular Agent, Chem. Biol. Drug Des. 86 (4) (2015) 410-423. https://doi.org/10.1111/cbdd.12527.

[25] J. Xie, C.T. Seto, A two stage click-based library of protein tyrosine phosphatase inhibitors, Bioorg. Med. Chem. 15(1) (2007) 15 458-473. https://doi.org/10.1016/j.bmc.2006.09.036.

[26] K.D. Thomas, A.V. Adhikari, I.H. Chowdhury, E. Sumesh, N.K. Pal, New quinolin-4-yl-1,2,3-triazoles carrying amides, sulphonamides and amidopiperazines as potential antitubercular agents, Eur. J. Med. Chem. 465 (6) (2011) 2503-2512. https://doi.org/10.1016/j.ejmech.2011.03.039.

[27] L. Pulipati, P. Yogeeswari, D. Sriram, S. Kantevari, Click-based synthesis and antitubercular evaluation of novel dibenzo[*b*,*d*]thiophene-1,2,3-triazoles with piperidine, piperazine, morpholine and thiomorpholine appendages, Bioorg. Med. Chem. Lett. 26 (11) 2016 2649-2654. https://doi.org/10.1016/j.bmcl.2016.04.015.

[28] H.N. Nagesh, K.M. Naidu, D. Harika Rao, J.P. Sridevi, D. Sriram, P. Yogeeswari, K.V. G.C. Sekhar, Design, synthesis and evaluation of 6-(4-((substituted-1*H*-1,2,3-triazol-4-yl)methyl)piperazin-1-yl)phenanthridine analogues as antimycobacterial agents, Bioorg. Med. Chem. Lett., 23 (24) 2013, 6805-6810. https://doi.org/10.1016/j.bmcl.2013.10.016.

[29] N. Boechat, V.F. Ferreira, S.B. Ferreira, M.L.G. Ferreira, F.C. da Silva, M.M. Bastos, M.S. Costa, M.S. Lourenço, A.C. Pinto, A.U. Krettli, A.C. Aguiar, B.M. Teixeira, N.V. da Silva, P.R. C. Martins, F.F.M. Bezerra, A.S. Camilo, G.P. da Silva and C.C.P. Costa, Novel 1,2,3-Triazole Derivatives for Use against *Mycobacterium tuberculosis* H37Rv (ATCC 27294) Strain, J. Med. Chem. 54 (17) (2011) 5988-5999. https://doi.org/10.1021/jm2003624.

[30] L.M. Lima, D.N. do Amaral, Beirut Reaction and its Application in the Synthesis of Quinoxaline-N,N'-Dioxides Bioactive Compounds, Rev. Virtual Quim, 5(67), 1075-1100. DOI: 10.5935/1984-6835.20130079

[31] A.A. Aziz, D. Gogoi, A.K. Chaliha, A.K. Buragohain, P. Trivedi, P.J. Saikia, P.S. Gehlot, A. Kumar, V. Chaturvedi, D. Sarma, Sekhar, Synthesis and biological evaluation of novel 1,2,3-triazole derivatives as anti-tubercular agents, Bioorg Med Chem Lett. 27(16) (2017) 3698-3703, https://doi.org/10.1016/j.bmcl.2017.07.008.

[32] K.M. Naidu, S. Srinivasarao, N. Agnieszka, A. Ewa, M.M. Krishna Kumar and K.V.G.C. Sekhar, Seeking potent anti-tubercular agents: Design, synthesis, anti-tubercular activity and docking study of various ((triazoles/indole)-piperazin-1-yl/1,4-diazepan-1-yl)benzo[*d*]isoxazole derivatives, Bioorg. Med. Chem. Lett., 26(9) (2016) 2245-2250,.https://doi.org/10.1016/j.bmcl.2016.03.059.

[33] J.D. Turnidge , J.H. Jorgensen, Manual of Clinical Microbiology. ed 7. Washington: American Society for Microbiology; 1999. Antimicrobial susceptibility testing: general considerations; pp. 1469–1473.

[34] H.V. Waterbeemd, E. Gifford, ADMET in silico modelling: towards prediction paradise? Nat. Rev. Drug Discov. 2(3) (2003) 192–204. https://doi.org/10.1038/nrd1032.

[35] Schrödinger Release 2019-1: QikProp, Schrödinger, LLC, New York, NY, 2019.

[36] Manual, Q. U. & Manual, Q. U. QikProp Descriptors and Properties PISA. 2–4 (2015).

[37] E. Lionta, G. Spyrou, D. Vassilatis and Z. Cournia, Structure-Based Virtual Screening for Drug Discovery: Principles, Applications and Recent Advances, Curr. Top. Med. Chem. 14 (16) (2014) 1923–1938. https://doi.org/10.2174/1568026614666140929124445.

[38] R.A. Friesner, J.L. Banks, R.B. Murphy, T.A. Halgren, J.J. Klicic, D.T. Mainz, M.P. Repasky, E.H. Knoll, M. Shelley, J.K. Perry and D.E. Shaw, Glide: A New Approach for Rapid, Accurate Docking and Scoring. 1. Method and Assessment of Docking Accuracy, J. Med. Chem. 47 (7) (2004) 1739–1749. https://doi.org/10.1021/jm0306430.

[39] T. Prakruti, N. Adhikari, S.A. Amin, T. Jha, B. Ghosh, Design, synthesis and biological screening of 2-aminobenzamides as selective HDAC3 inhibitors with promising anticancer effects, Eur. J. Pharm Sci. 124 (1) (2018) 165-181. https://doi.org/10.1016/j.ejps.2018.08.030.

Declaration of interest:

Authors declare no conflict of interest

Amongst 31 compounds, **8a** exhibited best anti-TB activity with MIC 12.5 µg/mL and unveiled favorable interactions with MTB DNA Gyrase.

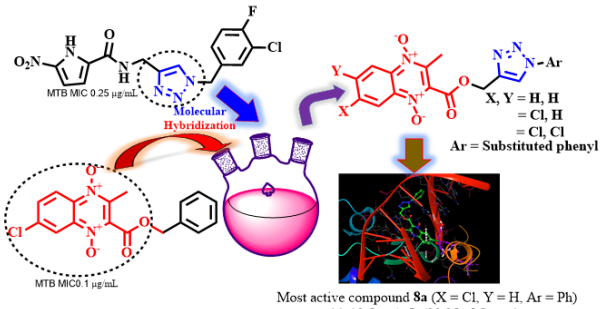

Most active compound **8a** (X = Cl, Y = H, Ar = Ph) with 12.5 µg/mL (30.35 µM) against MTB H37rv, spec. 210, and spec. 192

- ⇨ Thirty-one 1,2,3-triazole analogues of Quinoxaline-1,4-di-*N*-oxide were synthesized.
- ⇨ Screened the compounds against MTB H37Rv, spec. 192 and spec. 210.
- ⇨ **8a** exhibited good anti-TB activity with MIC 12.5 µg/mL against the tested strains.
- ⇨ Compounds were docked to MTB DNA Gyrase to know the binding interactions.
- ⇨ Most active compounds were less toxic against the normal HEK 293 cell line.